

## Increased antitumor efficacy of ginsenoside Rh<sub>2</sub> via mixed micelles: *in vivo* and *in vitro* evaluation

Xiaojing Xia<sup>a</sup>, Jin Tao<sup>a</sup>, Zhuwa Ji<sup>a</sup>, Chencheng Long<sup>a</sup>, Ying Hu<sup>a</sup> and Zhiying Zhao<sup>b</sup>

<sup>a</sup>Department of Pharmaceutics, Zhejiang Pharmaceutical College, Ningbo, PR China; <sup>b</sup>Department of Traditional Chinese Medicine, China Pharmaceutical University, Nanjing, PR China

### ABSTRACT

The aim of this work is to apply Solutol<sup>®</sup> HS15 and TPGS to prepare self-assembled micelles loading with ginsenoside Rh<sub>2</sub> to increase the solubility of ginsenoside Rh<sub>2</sub>, hence, improving the antitumor efficacy. Ginsenoside Rh<sub>2</sub>-mixed micelles (Rh<sub>2</sub>-M) were prepared by thin film dispersion method. The optimal Rh<sub>2</sub>-M was characterized by particle size, morphology, and drug encapsulation efficiency. The enhancement of *in vivo* anti-tumor efficacy of Rh<sub>2</sub>-M was evaluated by nude mice bearing tumor model. The solubility of Rh<sub>2</sub> in self-assembled micelles was increased approximately 150-folds compared to free Rh<sub>2</sub>. *In vitro* results demonstrated that the particle size of Rh<sub>2</sub>-M is  $74.72 \pm 2.63$  nm (PDI =  $0.147 \pm 0.15$ ), and the morphology of Rh<sub>2</sub>-M is spherical or spheroid, and the EE% and LE% are  $95.27 \pm 1.26\%$  and  $7.68 \pm 1.34\%$ , respectively. The results of *in vitro* cell uptake and *in vivo* imaging showed that Rh<sub>2</sub>-M could not only increase the cell uptake of drugs, but also transport drug to tumor sites, prolonging the retention time. *In vitro* cytotoxicity and *in vivo* antitumor results showed that the anti-tumor effect of Rh<sub>2</sub> can be effectively improved by Rh<sub>2</sub>-M. Therefore, Solutol<sup>®</sup> HS15 and TPGS could be used to entrapping Rh<sub>2</sub> into micelles, enhancing solubility and antitumor efficacy.

### ARTICLE HISTORY

Received 1 July 2020  
Revised 10 September 2020  
Accepted 14 September 2020

### KEYWORDS





Ginsenoside Rh<sub>2</sub>; mixed micelles; Solutol<sup>®</sup> HS15; TPGS; A549 cell; antitumor

### Introduction

Ginsenoside Rh<sub>2</sub> (Rh<sub>2</sub>) is a natural active component purified from *Rhizoma Ginseng*, which has many pharmacological activities, such as enhancing immunity (Lee et al., 2018), delaying aging (Chu et al., 2014), relaxing blood vessels, improving the insufficiency of cardiovascular and cerebrovascular blood supply (Lo et al., 2017) and anti-tumor efficiency (Chen & Qiu, 2015). Among them, the antitumor effect of Rh<sub>2</sub> has been an attractive topic recently. Studies show that Rh<sub>2</sub> can inhibit melanoma (Wang et al., 2017), glioma (Kim et al., 2007), liver cancer (Yang et al., 2016), breast cancer (Zare-Zardini et al., 2018), and lung cancer (An et al., 2013). Rh<sub>2</sub> inhibits tumor tissue growth by inhibiting the proliferation of tumor cells, inducing apoptosis (Zhuang et al., 2018), inhibiting tumor invasion (Li et al., 2015), migration and angiogenesis (Chen et al., 2018), and reversing/delaying multidrug resistance (Wen et al., 2015). The growth of tumor cells was interfered by regulating tumor microenvironment. Although the promising antitumor properties of Rh<sub>2</sub>, there is a fundamental challenge for the application of Rh<sub>2</sub>, extremely low solubility and rapid plasma elimination (Gu et al., 2009; Li et al., 2017). A few studies have reported that some drug delivery systems could enhance increase hydrophilicity and blood circulation of insoluble drugs by using a mixed micelles prepared with amphiphilic surfactants, and

the possible drug loading and antitumor effect still need to be improved (Chen et al., 2014; Jin et al., 2016).

Solutol<sup>®</sup> HS15 is a kind of nonionic surfactants with high safety, biocompatibility and commercial availability (Hou et al., 2016). It was originally developed as a parenteral formulation. For example, Solutol<sup>®</sup> HS15 was clinically developed as an osmotic enhancer for nasal spray (Williams et al., 2018). Recently, it is often used to improve the aqueous solubility of drug of Biopharmaceutical Classification System (BCS) Class II (Patel et al., 2011). However, studies on Solutol<sup>®</sup> HS15 are still limited, especially when used as a nanocarrier. It has been found that Solutol<sup>®</sup> HS15 can be assembled on lecithin to form lipid micelles to increase the solubility of insoluble drugs (Shaji & Varkey, 2016). TPGS is prepared by the esterification of vitamin E succinate with the hydroxyl of polyethylene glycol (PEG) 1000, which is FDA certified surfactant of polymer materials. And TPGS has many beneficial characteristics of high encapsulation efficiency and long internal circulation time. Besides, TPGS which forming a block copolymer micelle had the ability to inhibit the activity of P-gp (Dintaman & Silverman, 1999; Collnot et al., 2007; Choudhury et al., 2017; Jin et al., 2017; Liu et al., 2018). P-gp is one of the important proteins encoded by MDR1 gene and promotes the multidrug resistance of tumor cells. The main function of P-gp is to pump drugs out of cells, thereby

**CONTACT** Ying Hu  [pharmhawk@126.com](mailto:pharmhawk@126.com)  Department of Pharmaceutics, Zhejiang Pharmaceutical College, No. 888 East of Yinxian Road, Ningbo 315100, PR China; Zhiying Zhao  [zhaozhiying608@126.com](mailto:zhaozhiying608@126.com)  Department of Traditional Chinese Medicine, College of Traditional Chinese Pharmacy, China Pharmaceutical University, No. 639 Longmian Avenue, Jiangning District, Nanjing 211198, PR China

© 2020 The Author(s). Published by Informa UK Limited, trading as Taylor & Francis Group.  
This is an Open Access article distributed under the terms of the Creative Commons Attribution License (<http://creativecommons.org/licenses/by/4.0/>), which permits unrestricted use, distribution, and reproduction in any medium, provided the original work is properly cited.

limiting the injuring effect of drugs on tumor cells. TPGS binds to non-transporter active sites on P-gp, resulting in a change in the conformation of P-gp, and then lose the transshipment function of P-gp. Finally, the pump out of the drug by P-gp was inhibited, and the dosage of the needed drug was reduced, which resulted in higher tumor inhibition effect. Meanwhile it has been reported that based on the theory of synergistic effect, self-assembled micelles composed of two or more polymers exhibit preferable characteristics to micelles formed from only one surfactant (Hou et al., 2016).

Hence, in this paper, Solutol<sup>®</sup> HS15/TPGS-mixed micelles was prepared to increase the solubility and retention time of tumor site of Rh<sub>2</sub>, thus, enhancing the antitumor effect of Rh<sub>2</sub>. The mixed micelles containing Rh<sub>2</sub> were prepared by the thin-film dispersion method. The particle size, Zeta potential, and morphology were characterized by Malvern system particle size analyzer and transmission electron microscope, respectively. The *in vitro* release behavior of Rh<sub>2</sub>-mixed micelles (Rh<sub>2</sub>-M) was detected by dialysis method. MTT assay was used to detect the cytotoxicity of Rh<sub>2</sub>-M *in vitro* and its effect on cell migration, invasion and apoptosis were examined. *In vivo* imaging was used to visualize the enrichment ability and retention time of Rh<sub>2</sub>-M in tumor target. The tumor-bearing nude mice were used to evaluate the *in vivo* anti-tumor effect of Rh<sub>2</sub>-M.

## Materials and methods

### Materials

Ginsenoside Rh<sub>2</sub> of >98% purity was purchased from Nanjing Jingzhu Biotechnology, Jiangsu, China. Solutol<sup>®</sup> HS15 was purchased from BASF, Shanghai, China. TPGS was purchased from Aladdin, China. Methyl thiazolyl tetrazolium (MTT) and dimethyl sulfoxide (DMSO) were purchased from Nanjing Sunshine Biotechnology, Jiangsu, China. Coumarin-6 and DAPI were purchased from Sigma, Shanghai, China. DiR iodide (DiR) and the human lung adenocarcinoma cell line A549 was purchased from Nanjing KeyGen Biotech, Jiangsu, China. All reagents were of analytical grade except methanol, which was of chromatographic grade.

### Animals

Male athymic nude mice (22 ± 2g, SPF) were obtained from Changzhou Cavens Lab Animal Co., Ltd. (Changzhou, China, SCXK2011-0003). All mice were given distilled water and kept under pathogen-free conditions (25 ± 0.5 °C) for 3 days to acclimatize to the experimental environment. All animal experimental procedures were approved by the Institutional Animal Care and Use Committee (IACUC), Jiangsu Provincial Academy of Chinese Medicine's Experimental Animal Center. Prior to the tests, animals were fasted for 12 h and provided with only water.

### Preparation of drug-loaded micelles

The Solutol<sup>®</sup> HS15-TPGS-mixed micelles was prepared using the film dispersion method. In the preparation of Rh<sub>2</sub>-loaded mixed micelles, 17.5 mg Rh<sub>2</sub>, 140 mg Solutol<sup>®</sup> HS15 and 60 mg TPGS were dissolved in absolute ethyl alcohol (the ratio of Solutol<sup>®</sup> HS15 and TPGS is 7:3). Subsequently, volatile organic solvent was evaporated to dry in a rotary evaporator under 60 °C for 10 min, and dry film formed in the eggplant-shaped flask. 5 mL of Distilled water was added, and the solution was filtered with 0.45 μm filter membrane to remove the unencapsulated Rh<sub>2</sub>.

The preparation of coumarin-6-mixed micelles (C6-M) and DiR-mixed micelles (DiR-M) is the same as above method.

### Characterization of drug-loaded micelles

The zeta potential, hydrodynamic diameter and particle size distribution of the Rh<sub>2</sub>-M were measured by Malvern system (ZEN-3600, Malvern Instruments, Worcestershire, UK). Micellar solutions were filtered with a 0.45 μm filter prior to the measurement. All the values were the average of at least three parallel measurements.

Transmission electron microscopy (TEM) pictures of the copolymer micelles were captured on a transmission electron microscopy (TEM; JEM-200CX, JEOL, Tokyo, Japan). Briefly, A drop of Rh<sub>2</sub> micelles solution (1.0 mg/mL) was dipped into the copper grid, mixed with a drop of 2% (w/v) phosphotungstic acid. After the deposition, samples were observed under TEM.

The drug-loading efficiency (LE%) and encapsulation efficiency (EE%) were determined using a 4.6 mm × 250 mm Hypersil ODS C18 5.0 μm column (Thermo, Waltham, MA) by HPLC (Agilent 1260, Palo Alto, CA). Briefly, the Rh<sub>2</sub>-M solution was diluted with methanol to dissociate the micellar nanoparticles and centrifugation at 15,000 rpm for 15 min. Then the supernatant was filtrated by 0.45 μm filter membrane and the concentration of Rh<sub>2</sub> was determined by HPLC. The composition of the mobile phase was acetonitrile: water: phosphoric acid (65:35:0.2, v/v/v) with a flow rate of 1.0 mL/min at 35 °C. Quantitation was achieved using UV detection at 203 nm. A typical injection was 20 μL. The method was linear over a wide concentration range of 0.02–1.0 mg/mL. Assay method had been verified by methodology.

Then, use the following formula to calculate the LE% and EE%:

$$EE\% = \frac{\text{weight of } Rh_2 \text{ in micelles}}{\text{weight of the initial } Rh_2} \times 100\%$$

$$LE\% = \frac{\text{weight of } Rh_2 \text{ in micelles}}{\text{weight of micelles containing } Rh_2} \times 100\%$$

### In vitro release study

The *in vitro* release from the copolymer micelles Rh<sub>2</sub>-M were inspected using dialysis method (Wang et al., 2019). A phosphate buffer solution (PBS, pH = 7.4) including 0.5% Tween 80, which was chosen as a dissolution medium under

suitable sink conditions. 1.0 mL of free Rh<sub>2</sub> and aliquots of Rh<sub>2</sub> incorporated micelles (3.5 mg/mL of Rh<sub>2</sub>) were transferred into the dialysis bags (molecular weight cutoff size 3,500 Da), which were tightened and put into 100 mL dissolution medium. Then concussion in a thermostatic oscillator (37 ± 0.5 °C, 100 rpm), 1 mL dissolution medium was taken out in predetermined interval (0, 0.25, 0.5, 1, 4, 8, 12, 24, and 48 h), and replaced with an equal volume of fresh medium. The concentration of Rh<sub>2</sub> was measured by HPLC and *in vitro* Rh<sub>2</sub> release profiles were plotted with cumulative drug release as a function of time. Experiments were conducted in triplicate.

### In vitro cytotoxicity analysis

Inhibitory effect of Rh<sub>2</sub> and Rh<sub>2</sub>-M on proliferation of A549 cells was detected by MTT assay (Quandt et al., 2014). In logarithmic growth phase, A549 cells were digested with trypsin. Single cell suspension was obtained from 10% fetal bovine serum DMEM. The cells were diluted to 4 × 10<sup>4</sup>/mL and inoculated into 96-well cell culture plate with 100 μL culture medium in each hole. PBS was added to the bottom and both sides of the cells. A549 cells were cultured at 37 °C in a 5% CO<sub>2</sub> atmosphere for 24 h, subsequently, free Rh<sub>2</sub> and Rh<sub>2</sub>-M diluted with different concentrations were added into the culture medium. After 24 h of incubation, the culture medium was removed and added with 100 μL MTT solution (0.5 mg/mL) and incubated for 4 h. MTT was discarded and then dimethyl sulfoxide solution (DMSO, 100 μL) was added. The medium was shaken at a speed of 50 rpm for 10 min. The absorbance of the sample was measured at 570 nm using the microplate reader (Bio-Rad Laboratories, Hercules, CA), and the IC<sub>50</sub> was calculated. Six parallel composite holes were set for each concentration:

$$\text{Cell viability} = \frac{A_{\text{sample}} - A_{\text{blank}}}{A_{\text{control}} - A_{\text{blank}}} \times 100\%$$

### Cellular uptake

Coumarin-6 was used as a model Active pharmaceutical ingredient for cellular uptake (Rivolta et al., 2011). A549 cells in logarithmic growth phase were inoculated with a density of 1 × 10<sup>5</sup>/well on a 24 well culture plate, incubated for 24 h to make A549 cells adhere to the wall. After the old culture medium was abandoned, coumarin-6 and C6-M were added respectively and cultured for 4 h. Subsequently, cold PBS was added to terminate cell uptake and the cells were flushed by PBS for 3 times. Immobilized cells at 4 °C for 30 min with anhydrous ethanol and stained with DAPI (5 μg/mL). The cells were incubated for 10 min and washed with PBS for 2 times (Yang et al., 2017). The uptake of cells was observed under fluorescence microscope.

### Cell migration

Scratch assay was widely available format to study cell migration (Hulkower & Herber, 2011). The cells in logarithmic

growth period were digested and inoculated into the six-hole plate. when the cell aggregation was about 80%, the sterile gun head was used to draw the line evenly in the six-hole plate. After the floating cells were washed off with PBS, the fresh culture medium containing free Rh<sub>2</sub> (26.48 μg/mL of Rh<sub>2</sub>) and Rh<sub>2</sub>-M (26.48 μg/mL of Rh<sub>2</sub>) were replaced and cultured in a cell incubator. After 24 h of incubation, the cells were taken out and photographed (magnification multiple 100), the cell migration distance was measured.

### In vivo imaging

The nude mice of the same weight were inoculated A549 cells on their backs. After the tumor grew to 60 mm, DiR fluorescent dye (0.5 mg/mL of DiR) and DiR-mixed micelles (0.5 mg/mL of DiR) were injected into the tail vein, respectively (Jiang et al., 2012). The nude mice were anesthetized at 0.5 h, 2 h, 4 h, 8 h, 12 h, and 24 h, and the fluorescence intensity of tumor sites and organs *in vivo* were detected on an *in vivo* imaging system (NightOWLII LB983; Berthold, Wildbad, Germany). After 24 h, the nude mice were euthanized, planed and the heart, liver, spleen, lung, kidney, and tumor were collected to detect fluorescent expression on the living imager.

### In vivo antitumor activity

The logarithmic A549 cells were inoculated on the back of nude mice (22 ± 2 g). When the tumor reached about 50 mm, the nude mice were randomly grouped. Nude mice were randomly allocated to model group (0.2 mL of normal saline), positive drug group (2 mg/kg of cisplatin), Rh<sub>2</sub> group (15 mg/kg of Rh<sub>2</sub>), and Rh<sub>2</sub>-M group (15 mg/kg of Rh<sub>2</sub>). Tail vein injections were administered for 18 days, and dosing five times (Yang et al., 2016). Weight and tumor size measured before each dose. The nude mice were euthanized on the third day after the last administration, and the tumor was taken and weighed and photographed. The tumor volume (V) is calculated as:  $V = a \times b^2/2$ , where *a* and *b* are the length and width of the tumor, respectively. According to the above measurements, the relative tumor volume was calculated, and antitumor activity was evaluated by the relative tumor growth rate (T/C):

$$\text{RTV} = V_t/V_0$$

$$\text{T/C} = T_{\text{RTV}}/C_{\text{RTV}} \times 100\%$$

where *V*<sub>0</sub> is the tumor size at 0 day; *V*<sub>*t*</sub> is the tumor volume at each measurement; *T*<sub>RTV</sub> is the RTV of the treatment groups; and *C*<sub>RTV</sub> is the RTV of the control group.

The tumor and the liver of each group were kept in 10% formaldehyde bag. The tissue was then embedded in a wax block for easy slicing. After two xylene and gradient alcohol (100%, 90%, 80%, and 70%) dew axing and hydration, the cut wax sheet is dyed in sequence by using wood essence and eosin, and finally the wax sheet is sealed with a neutral gum. Tissue samples were observed and photographed microscope.

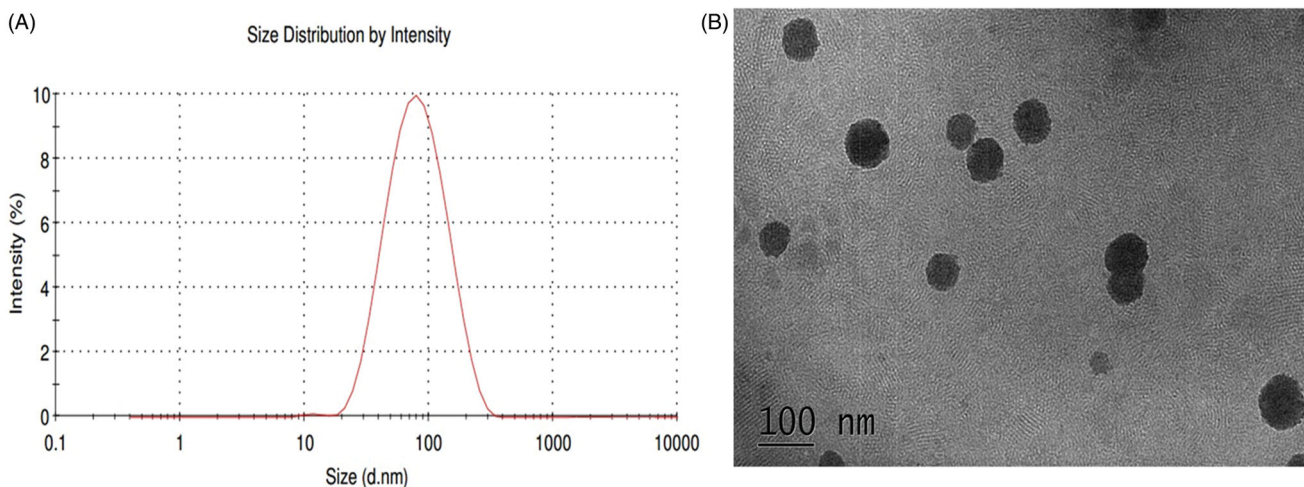


Figure 1. Size distribution and TEM of Rh<sub>2</sub>-mixed micelles.

### Histological studies

The samples of and livers in studies were removed from mice and post fixed in 4% neutral formaldehyde, then embedded in paraffin wax for pathological cut sheet. Sections were stained with hematoxylin and eosin and observed with an upright microscope (Eclipse Ni-U, Nikon, Japan).

### Statistical analysis

All data are represented by mean  $\pm$  SD, and SPSS version 19.0 (SPSS Inc., Chicago, IL) was used to detect the significance between groups ( $p < .05$ ). Differences between two groups were assessed using Student's *t*-test.

## Results

### Mixed micelle formulation and characterization

The Rh<sub>2</sub>-mixed micelle solution prepared by thin-film dispersion method was clarified without obvious flocculent precipitation and had light blue emulsion light. The optimized formulation is Solutol<sup>®</sup> HS15: TPGS = 7: 3, and the LE% and EE% are  $7.68 \pm 1.34\%$  and  $95.27 \pm 1.26\%$ , respectively. The concentration of Rh<sub>2</sub> in Rh<sub>2</sub>-M is  $3.33 \pm 0.04$  mg/mL, which is an approximately 150 time higher than that of Rh<sub>2</sub> in water ( $23.1 \pm 1.5$   $\mu$ g/mL) (Souza et al., 2019). As seen in Figure 1, the Rh<sub>2</sub>-M exhibited spherical or spheroid. The particle size of the prepared micelles was uniform (PDI =  $0.147 \pm 0.15$ ), the average particle size was  $74.72 \pm 2.63$  nm (Figure 1(A)). The  $\zeta$  potential of the Rh<sub>2</sub>-M was  $-26.2 \pm 0.9$  mV, which indicated the high ability to hinder the probability of coalescence and thereby maintaining the homogeneity of nanodroplets (Honary & Zahir, 2013). Therefore, Rh<sub>2</sub>-M is prepared successfully with almost spherical and uniform shapes and increased the solubility.

### In vitro release of Rh<sub>2</sub>-loaded mixed micelles

The slow release of drug by sustained-release preparations is helpful to retard the absorption rate of drug into the

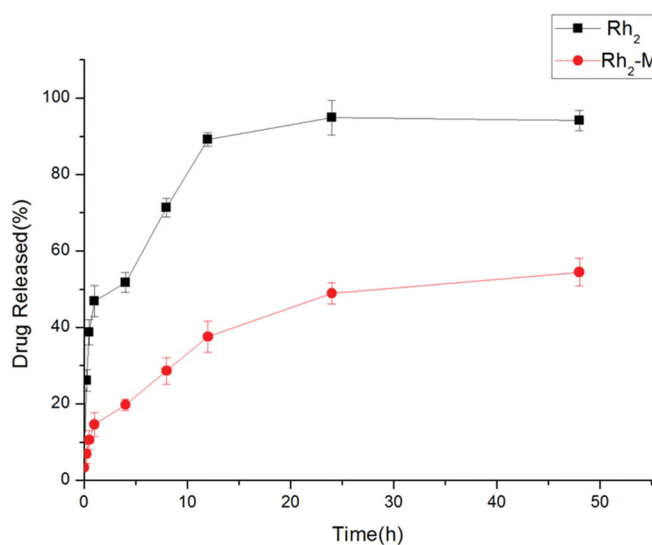


Figure 2. *In vitro* release profiles of Rh<sub>2</sub>-M and free drug, data represent the mean  $\pm$  SD ( $n = 6$ ).

body, thus, making the drug play a better therapeutic effect. A sudden release occurs at the initial stage of Rh<sub>2</sub>-M release, followed by a sustained and slow release of the drug, and sustained release of the Rh<sub>2</sub>-M within 48 h. Rh<sub>2</sub> has released 51.73% in 4 h, and completely released in 24 h (Figure 2), demonstrating that Rh<sub>2</sub>-M has a certain slow-release effect, which may enhance the antitumor efficacy of Rh<sub>2</sub>.

### In vitro cytotoxicity of micelles

As shown in Figure 3, Rh<sub>2</sub> and Rh<sub>2</sub>-M showed cytotoxicity against A549 cell line, and the latter exhibited higher cell cytotoxicity. Respectively, the results showed that the IC<sub>50</sub> of Rh<sub>2</sub> and Rh<sub>2</sub>-M were  $26.48 \pm 2.13$   $\mu$ g/mL and  $21.71 \pm 1.85$   $\mu$ g/mL, which suggest that Rh<sub>2</sub>-M can enhance the inhibitory effect of Rh<sub>2</sub> on lung cancer cells ( $p < .05$ ). The IC<sub>50</sub> of blank micelles was greater than 100  $\mu$ g/mL. It was inferred that the nanocarrier had good biocompatibility.

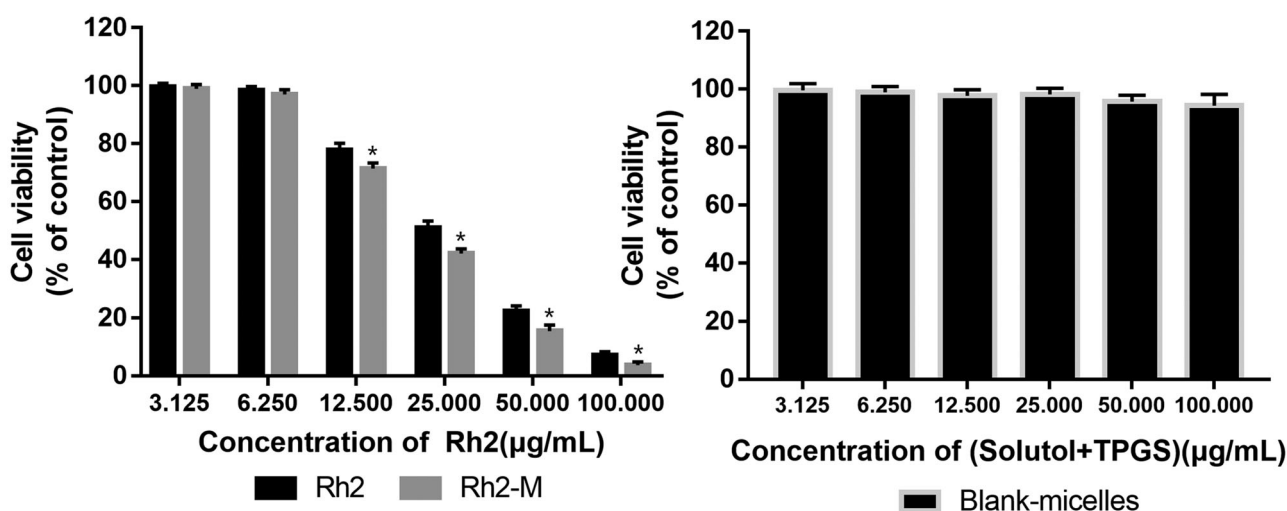


Figure 3. Cell cytotoxicity in A549 Cells. Note: data shown represent the mean values of six experiments  $\pm$  SD. \* $p < .05$ .

### Cellular uptake

The fluorescent dye coumarin-6 (C6) is often used to replace insoluble drugs in order to investigate whether nano pharmaceuticals can improve the efflux of drugs. In this paper, coumarin-6 was coated with mixed micelles composed of Solutol<sup>®</sup> HS15 and TPGS (C6-M), and then A549 cells was cultured in serum-free medium containing C6 and C6-M for 4 h. As depicted in Figure 4, green fluorescence represents C-6, blue fluorescence represents nucleus. At the same time, the fluorescence intensity of C6-M can be used as preliminary judgments of the ability of cell uptake of drugs. Four hours later, the green fluorescence intensity of C6-M was significantly stronger than that of C6, indicating that the mixed micelles with Solutol<sup>®</sup> HS15 and TPGS could enhance the cell uptake of drugs. The possible reasons were the small size of nanoparticle and the amphiphilic carrier, in addition to this, TPGS might inhibit the activity of P-gp and then the cellular uptake to C6 was improved significantly.

### Inhibitory effect of Rh<sub>2</sub>-M on cell migration

The migration of tumor cells is the process that tumor cells invade lymphatic vessels, blood vessels, or body cavities from their primary site and the tumor cells continue to grow, forming a tumor as the primary tumor. Inhibition of tumor cell migration via drugs can effectively prevent tumor deterioration, which is one of the important indexes to evaluate the efficacy of antitumor drugs. Compared to blank control, the migration length of A549 cells was shortened after Rh<sub>2</sub>-M ( $159.77 \pm 3.80 \mu\text{m}$ ) and Rh<sub>2</sub> ( $109.25 \pm 4.84 \mu\text{m}$ ,  $p < .05$ ) treatment, respectively (Figure 5).

### In vivo imaging

As shown in Figure 6, the fluorescence expression of DiR dye group is mainly concentrated in the liver. In the DiR-M group, the fluorescence was displayed at the tumor site at 6 h and showed an increasing tendency with the time lapsed.

After 24 h of euthanasia, the nude mice were euthanized and the heart, liver, spleen, lung, kidney, and tumor were taken to take pictures. The results showed that there was still fluorescence expression in the tumor site of DiR-M group 24 h later. These results indicated that Rh<sub>2</sub>-M can increase the concentration and retention time of Rh<sub>2</sub> in tumor site, thus enhancing the tumor inhibition effect of Rh<sub>2</sub> *in vivo*.

### In vivo antitumor activity

The *in vivo* antitumor effect of Rh<sub>2</sub>-M *via* nude mice bearing tumor model was investigated (Figure 7). The tumor volume in the positive group was significantly lower than that in the control group during the third administration ( $p < .05$ ). At the same time, the body weight of the positive group decreased gradually with the increase of administration times. It shows that cisplatin has a significant inhibitory effect on lung cancer, but with serious side effects on the body weight. Compared with the model group, Rh<sub>2</sub> and Rh<sub>2</sub>-M have inhibitory effect on the growth of lung cancer tumor, and with the prolongation of administration time, the inhibitory effect is enhanced. After the fifth dose, the tumor volume of Rh<sub>2</sub>-M group was significantly lower than that of model group ( $p < .05$ ). The weight of nude mice in Rh<sub>2</sub> and Rh<sub>2</sub>-M groups was not significantly different from that in model group, indicating the safety of Rh<sub>2</sub> and Rh<sub>2</sub>-M.

At the end of the experiment, the nude mice were planned, and the tumors were weighed. Results as shown in the table, the tumor weight of Rh<sub>2</sub>-M was significantly lower than that of the model group. Therefore, the above results indicate that Rh<sub>2</sub> has a certain inhibitory effect on the growth of lung cancer, and Rh<sub>2</sub>-M can enhance the inhibitory effect of Rh<sub>2</sub> on lung cancer.

### Histological studies

The results of hematoxylin-eosin (HE) staining showed that the tumor cells in the positive group and the Rh<sub>2</sub>-M group had different degrees of necrosis, while the tumor cells in

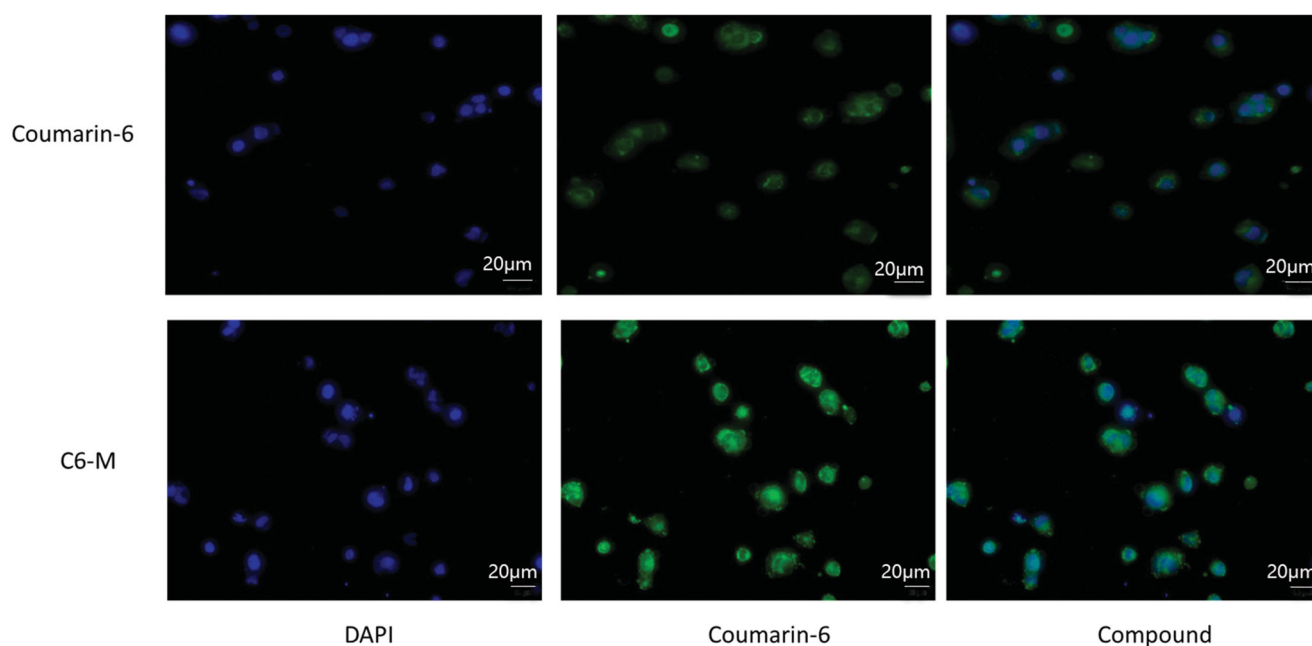


**Figure 4.** Cell uptake of coumarin-6 (C6) and C6-M by A549 cells observed by fluorescence inverted microscope.

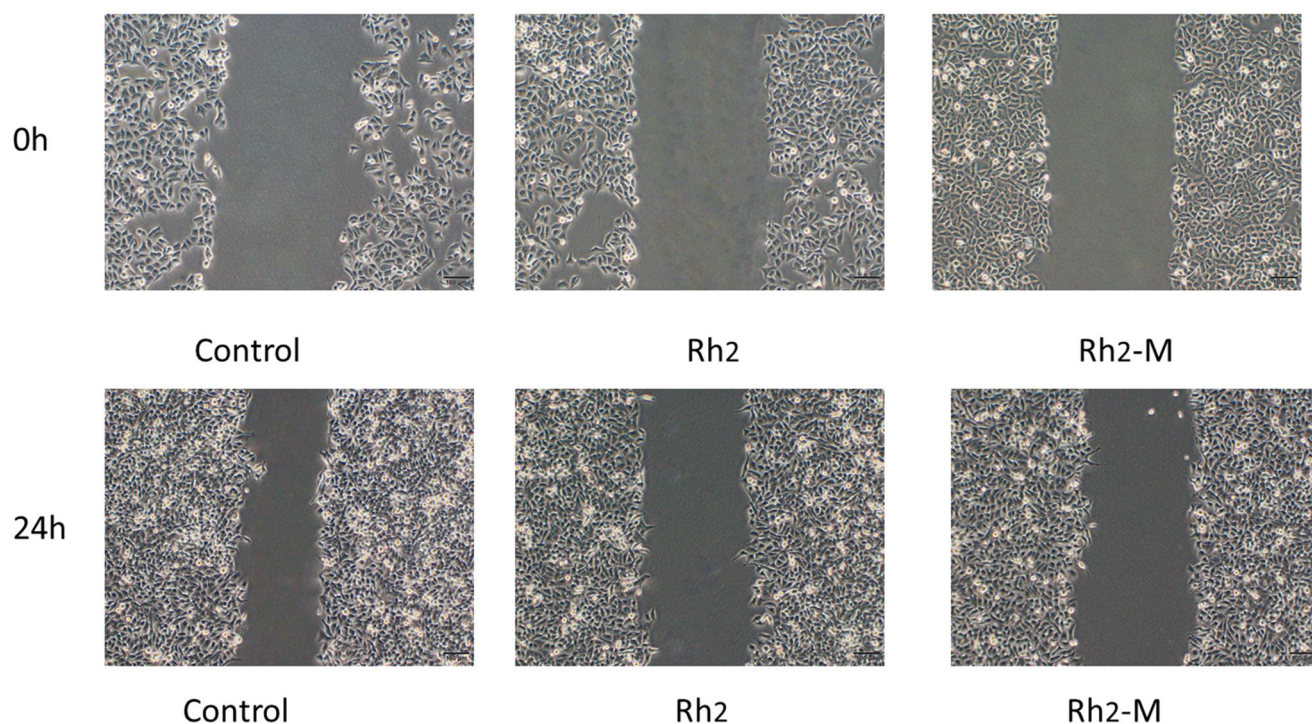


**Figure 5.** Representative micrographs pictures of A549 scratch assays at 0 h and 24 h.

the positive group and the Rh<sub>2</sub>-M group had slight apoptosis, which further indicated that Rh<sub>2</sub>-M had inhibitory effect on lung cancer cells (Figure 8).

The liver is the main metabolic organ of the body. Drugs must enter the systemic circulation through the liver before distributed to the diseased site. Therefore, the liver is greatly affected by the side effects of drugs. The toxic and side effects of anti-tumor drugs and new nano-preparations on liver should also be included in the safety evaluation. The results of Figure 8 showed that there were multiple focal

necroses (moderate necrosis) in the liver tissue of the positive group, and the hepatocytes disappeared in the necrotic area. There was no obvious hepatic lesion in Rh<sub>2</sub> and Rh<sub>2</sub>-M groups.

## Discussion

Rh<sub>2</sub> is one of the most effective monomers in ginsenosides. However, due to the poor solubility of Rh<sub>2</sub>, its clinical application is restricted. In recent years, researchers have

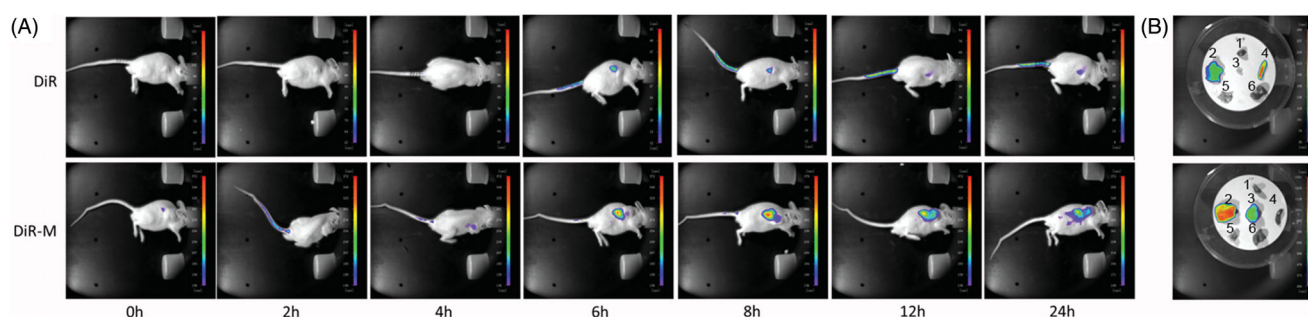


**Figure 6.** Confocal laser scanning microscopy (CLSM) of (A) tumor-bearing nude mice after administration of free DiR and DiR mixed micelles at 0, 2, 4, 6, 8, 12, and 24 h and (B) mice main organs after 24 h. (1) Heart, (2) liver, (3) tumor, (4) spleen, (5) lung, and (6) kidney.

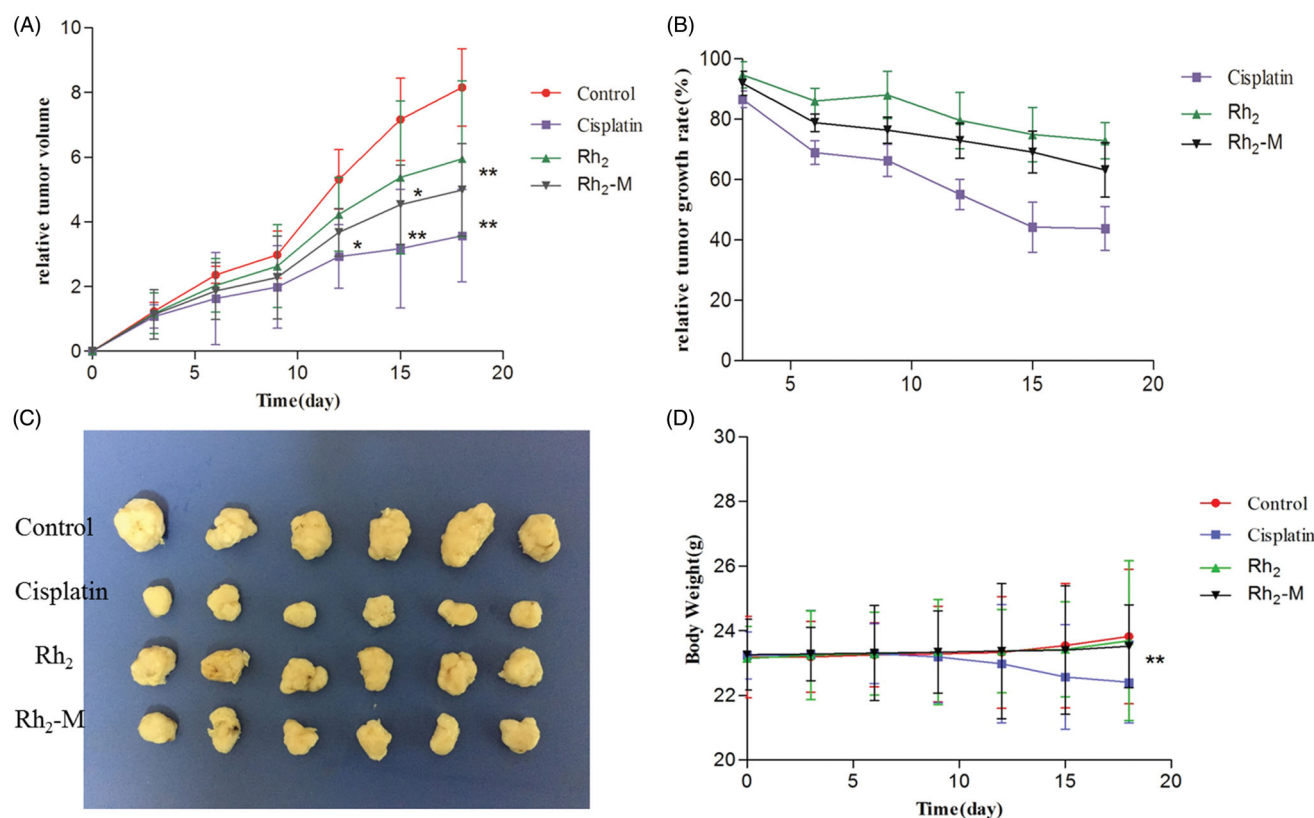


**Figure 7.** Effect on the inhibition of tumor growth of cisplatin, Rh<sub>2</sub>, Rh<sub>2</sub>-M and control group in tumor-bearing nude mice. Data represent the mean  $\pm$  SD ( $n = 6$ ). (A) Relative tumor volume; (B) relative tumor growth rate; (C) image of tumor; (D) body weight.

developed a variety of nano pharmaceuticals to improve the solubility of Rh<sub>2</sub>, such as self-microemulsions (Yang et al., 2017), nanoparticles (Singh et al., 2017; Kim et al., 2019), liposome-based delivery systems (Yang et al., 2016), and pH-sensitive mixed micelles (Zhuang et al., 2018).

Polymer micelles can be used as carriers of antineoplastic drugs to effectively improve drug defects. The polymer carriers spontaneously form micelles with a hydrophobic core and a hydrophilic shell in water. Hydrophobic drugs are encapsulated into the core and delivered to tumor targets, while reducing accumulation in other areas and protecting the drug from inactivation in biological media, thus the anti-neoplastic effect of the drug is improved. In this paper, Rh<sub>2</sub>-mixed micelles were successfully prepared by the thin film dispersion method. The size of the prepared Rh<sub>2</sub>-M particles is uniform; the morphology is spherical or spherical, and the average particle size is  $74.72 \pm 2.63$  nm. Encapsulation

efficiency and drug loading efficiency of Rh<sub>2</sub>-M were  $95.27 \pm 1.26\%$  and  $7.68 \pm 1.34\%$ , respectively. The results of *in vitro* release showed that Rh<sub>2</sub>-M was released slowly within 48 h, and the accumulative release percentage was  $54.42 \pm 3.21\%$ . Therefore, the prepared Rh<sub>2</sub>-M can effectively increase the solubility of Rh<sub>2</sub> and has a certain slow-release effect, which lays a certain foundation for increasing the anti-tumor effect of Rh<sub>2</sub>.

The hemolysis test, stability in physiological conditions, and shelf stability were evaluated further. The results of hemolysis test (Song et al., 2014) showed that the hemolysis percentage of Solutol:TPGS (7:3) was 0.73% (0.5 mg/mL of mix nanocarrier), while the hemolysis percentage of Rh<sub>2</sub>-M (0.1 mg/mL of Rh<sub>2</sub>) was 1.56% ( $n = 3$ ). The Rh<sub>2</sub>-loaded Solutol TPGS mix micelles were mixed with appropriate volumes containing 10%vol% fetal bovine serum (Zhang et al., 2014). The diluted samples were incubated at 37 °C. Samples were

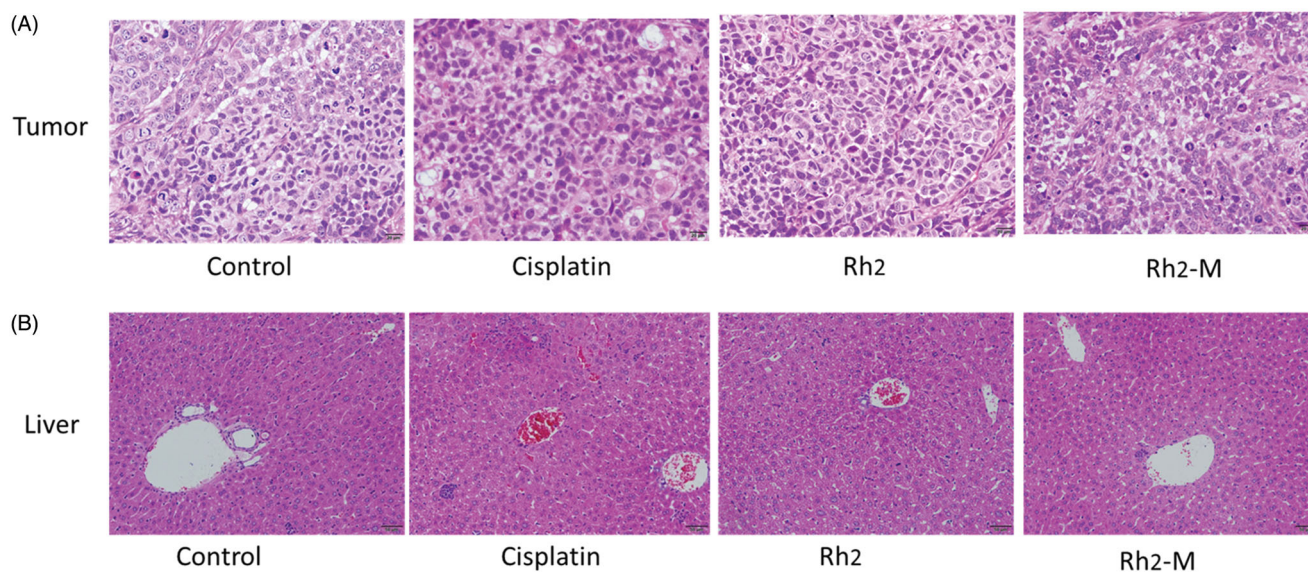


**Figure 8.** Histopathological section of the tumor and liver treated with saline solution, cisplatin, Rh<sub>2</sub>, and Rh<sub>2</sub>-M.

taken to determine the particle size at 2, 4, 6, 8, 12 h, and 24 h. The experiments were repeated three times, and the average values are reported ( $n = 3$ ). There was a little increasing in particle size ( $78.91 \pm 2.15$  nm after storage). And  $93.3 \pm 1.6\%$  of the Rh<sub>2</sub> content in the mix micelles remained. Rh<sub>2</sub>-M could be preserved for more than 21 days at 4° C and 5–6 days at 25° C. It can be inferred that the mix micelles have less hemolysis, good biocompatibility, and Rh<sub>2</sub>-M are stable in physiological conditions.

In the further study, MTT cell proliferation assay and cell migration test were used to evaluate the cytotoxicity of Rh<sub>2</sub> and check whether Rh<sub>2</sub>-M could increase the effect. The results showed that the IC<sub>50</sub> of Rh<sub>2</sub>-M was  $21.71 \pm 1.85$  μg/mL, which was superior to that of IC<sub>50</sub> of Rh<sub>2</sub> ( $26.48 \pm 2.13$  μg/mL). And Rh<sub>2</sub>-M could enhance the inhibitory effect of Rh<sub>2</sub> on the migration of lung cancer A549 cells. And the blank Solutol<sup>®</sup>HS15 and TPGS self-assembled micelles have no obvious cytotoxicity to A549 cells. The results suggest that Rh<sub>2</sub>-M enhances the proliferation of A549 cells by Rh<sub>2</sub>. Further studies have found that Rh<sub>2</sub> has a good inhibitory effect on tumor cell migration, and Rh<sub>2</sub>-M can enhance this inhibitory effect.

It has been found that TPGS can inhibit drug delivery mediated by P-gp and inhibit multidrug resistance (MDR) (Gao et al., 2016). As a result, the concentration of the drugs entered the cell is increased, and the antitumor effect of the drugs increases. On the other hand, it was found that micelles with particle size below 200 nm could avoid being swallowed by reticuloendothelial system and make more drugs enter the target site (Lai et al., 2010). The results of *in vivo* imaging showed that the fluorescence expression of DiR dye encapsulated by micelles of Solutol<sup>®</sup>HS15 and TPGS was much higher than that of free DiR dye, and the retention time of DiR-M in tumor site was more than 24 h.

The increase of cell uptake and drug concentration in tumor site directly leads to the increase of antitumor effect of Rh<sub>2</sub>. Tumors bearing nude mice were selected to evaluate

the antitumor effect *in vivo*. The statistical results showed that the tumor inhibition rate of Rh<sub>2</sub>-M was  $38.84 \pm 5.92\%$ , which was significantly higher than that of the model group ( $p < .05$ ). Rh<sub>2</sub>-M had no obvious inhibitory effect on the body weight of nude mice and no obvious toxicity to the liver, while the weight loss of the positive group was obvious. Herein, the prepared Rh<sub>2</sub>-M can enhance the anti-tumor effect of Rh<sub>2</sub> and has no significant toxicity to the body, thus it is a potential and safe anti-tumor nanometer preparation.

## Conclusion

The solubility and the antitumor effect of Rh<sub>2</sub> were enhanced by Rh<sub>2</sub>-M using Solutol<sup>®</sup>HS15 and TPGS. The LE% and multi-drug resistance of Rh<sub>2</sub> could be increased by Rh<sub>2</sub>-M. Meanwhile, Rh<sub>2</sub> was released in a sustained behavior from Rh<sub>2</sub>-M, and Rh<sub>2</sub>-M could directly increase Rh<sub>2</sub> uptake and tumor site concentration. The experimental results of anti-tumor effect *in vivo* and *in vitro* proved that the mixed micelle system composed of Solutol<sup>®</sup>HS15 and TPGS could not only improve the solubility of drugs, but also increase the concentration and retention time of drugs in the tumor site, and finally increase the anti-tumor effect. Thus, this system could serve as a promising carrier of Rh<sub>2</sub> for cancer therapy.

## Disclosure statement

The authors report no conflict of interest.

## Funding

This work was supported by the National Natural Science Foundation of China under Grant [81803462] and the Natural Science Foundation of Ningbo under Grant [2018A610433].



## References

- An IS, An S, Kwon KJ, et al. (2013). Ginsenoside Rh2 mediates changes in the microRNA expression profile of human non-small cell lung cancer A549 cancer A549 cells. *Oncol Rep* 29:523–8.
- Chen D, Yu H, Mu H, et al. (2014). Novel multicore niosomes based on double pH-sensitive mixed micelles for Ginsenoside Rh2 delivery. *Artif Cells Nanomed Biotechnol* 42:205–9.
- Chen W, Qiu Y. (2015). Ginsenoside Rh2 targets EGFR by up-regulation of miR-491 to enhance anti-tumor activity in hepatitis B virus-related hepatocellular carcinoma. *Cell Biochem Biophys* 72:325–31.
- Chen Y, Shang H, Zhang S, et al. (2018). Ginsenoside Rh2 inhibits proliferation and migration of medulloblastoma Daoy by down-regulation of microRNA-31. *J Cell Biochem* 119:6527–34.
- Choudhury H, Gorain B, Pandey M, et al. (2017). Recent advances in TPGS-based nanoparticles of docetaxel for improved chemotherapy. *Int J Pharm* 529:506–22.
- Chu JM, Lee DK, Wong DP, et al. (2014). Ginsenosides attenuate methylglyoxal-induced impairment of insulin signaling and subsequent apoptosis in primary astrocytes. *Neuropharmacology* 85:215–23.
- Collnot EM, Baldes C, Wempe MF, et al. (2007). Mechanism of inhibition of P-glycoprotein mediated efflux by vitamin E TPGS: influence on ATPase activity and membrane fluidity. *Mol Pharm* 4:465–74.
- Dintaman JM, Silverman JA. (1999). Inhibition of P-glycoprotein by D-alpha-tocopheryl polyethylene glycol 1000 succinate (TPGS). *Pharm Res* 16:1550–6.
- Gao L, Wang X, Ma J, et al. (2016). Evaluation of TPGS-modified thermo-sensitive Pluronic PF127 hydrogel as a potential carrier to reverse the resistance of P-gp-overexpressing SMMC-7721 cell lines. *Colloids Surf B Biointerfaces* 140:307–16.
- Gu Y, Wang GJ, Sun JG, et al. (2009). Pharmacokinetic characterization of ginsenoside Rh2, an anticancer nutrient from ginseng, in rats and dogs. *Food Chem Toxicol* 47:2257–68.
- Honary S, Zahir F. (2013). Effect of zeta potential on the properties of nano-drug delivery systems – a review (Part 1). *Tropical J Pharm Res* 12:255–64.
- Hou J, Sun E, Sun C, et al. (2016). Improved oral bioavailability and anticancer efficacy on breast cancer of paclitaxel via Novel Soluplus®-Solutol® HS15 binary mixed micelles system. *Int J Pharm* 512: 186–93.
- Hou J, Wang J, Sun E, et al. (2016). Preparation and evaluation of icarisi- side II-loaded binary mixed micelles using Solutol HS15 and Pluronic F127 as carriers. *Drug Deliv* 23:3248–56. *Nov*
- Hulkower KI, Herber RL. (2011). Cell migration and invasion assays as tools for drug discovery. *Pharmaceutics* 3:107–24.
- Jiang T, Zhang Z, Zhang Y, et al. (2012). Dual-functional liposomes based on pH-responsive cell-penetrating peptide and hyaluronic acid for tumor-targeted anticancer drug delivery. *Biomaterials* 33:9246–58.
- Jin X, Li M, Yin L, et al. (2017). Tyroservatide-TPGS-paclitaxel liposomes: tyroservatide as a targeting ligand for improving breast cancer treatment. *Nanomedicine* 13:1105–15.
- Jin X, Zhang Y, Zhang Z, et al. (2016). Juglone loaded Poloxamer 188/ phospholipid mixed micelles evaluated in vitro and in vivo in breast cancer. *Int J Pharm* 515:359–66.
- Kim SY, Kim DH, Han SJ, et al. (2007). Repression of matrix metalloproteinase gene expression by ginsenoside Rh2 in human astrogloma cells. *Biochem Pharmacol* 74:1642–51.
- Kim YJ, Perumalsamy H, Castro-Aceituno V, et al. (2019). Photoluminescent and self-assembled hyaluronic acid-zinc oxide-ginsenoside Rh2 nanoparticles and their potential caspase-9 apoptotic mechanism towards cancer cell lines. *Int J Nanomed* 14:8195–208.
- Lai J, Chang Y, Yen H, et al. (2010). Multifunctional doxorubicin/superparamagnetic iron oxide-encapsulated Pluronic F127 micelles used for chemotherapy/magnetic resonance imaging. *J Appl Phys* 107:969.
- Lee H, Lee S, Jeong D, et al. (2018). Ginsenoside Rh2 epigenetically regulates cell-mediated immune pathway to inhibit proliferation of MCF-7 breast cancer cells. *J Ginseng Res* 42:455–62.
- Li P, Zhou X, Qu D, et al. (2017). Preliminary study on fabrication, characterization and synergistic anti-lung cancer effects of self-assembled micelles of covalently conjugated celastrol-polyethylene glycol-ginsenoside Rh2. *Drug Deliv* 24:834–45.
- Li S, Gao Y, Ma W, et al. (2015). Ginsenoside Rh2 inhibits invasiveness of glioblastoma through modulation of VEGF-A. *Tumor Biol* 23:1–6.
- Liu T, Liu X, Xiong H, et al. (2018). Mechanisms of TPGS and its derivatives inhibiting P-glycoprotein efflux pump and application for reversing multidrug resistance in hepatocellular carcinoma. *Polym Chem* 9: 1827–39.
- Lo SH, Hsu CT, Niu HS, et al. (2017). Ginsenoside Rh2 improves cardiac fibrosis via PPAR $\delta$ -STAT3 signaling in type 1-like diabetic rats. *IJMS* 18:1364.
- Patel J, Kevin G, Patel A, et al. (2011). Design and development of a self-nanoemulsifying drug delivery system for telmisartan for oral drug delivery. *Int J Pharm Investig* 1:112–8.
- Quandt D, Jasinski Bergner S, Müller U, et al. (2014). Synergistic effects of IL-4 and TNF $\alpha$  on the induction of B7-H1 in renal cell carcinoma cells inhibiting allogeneic T cell proliferation. *J Transl Med* 12:151
- Rivolta I, Panariti A, Lettiero B, et al. (2011). Cellular uptake of coumarin-6 as a model drug loaded in solid lipid nanoparticles. *J Physiol Pharmacol* 62:45–53.
- Shaji J, Varkey D. (2016). Meloxicam-loaded phospholipid/solutol® HS15 based mixed nanomicelles: preparation, characterization, and in vitro antioxidant activity. *Pharm Nanotechnol* 4:167–90.
- Singh P, Kim YJ, Singh H, et al. (2017). In situ preparation of water-soluble ginsenoside Rh2-entrapped bovine serum albumin nanoparticles: in vitro cytocompatibility studies. *Int J Nanomed* 12:4073–84.
- Song Z, Zhu W, Liu N, et al. (2014). Linolenic acid-modified PEG-PCL micelles for curcumin delivery. *Int J Pharm* 471:312–21.
- Souza J. B d, Souza J. d, Castro L. M L d, et al. (2019). Evaluation of the losartan solubility in the biowaver context by shake-flask method and intrinsic dissolution. *Pharm Dev Technol* 24:283–92.
- Wang M, Yan SJ, Zhang HT, et al. (2017). Ginsenoside Rh2 enhances the antitumor immunological response of a melanoma mice model. *Oncol Lett* 13:681–5.
- Wang W-J, Huang Y-C, Su C-M, et al. (2019). Multi-functional drug carrier micelles with anti-inflammatory drug. *Front Chem* 7:93
- Wen X, Zhang HD, Zhao L, et al. (2015). Ginsenoside Rh2 differentially mediates microRNA expression to prevent chemoresistance of breast cancer. *Asian Pac J Cancer Prev* 16:1105–9.
- Williams AJ, Jordan F, King G, et al. (2018). In vitro and preclinical assessment of an intranasal spray formulation of parathyroid hormone PTH 1-34 for the treatment of osteoporosis. *Int J Pharm* 535:113–9.
- Yang F, Zhou J, Hu X, et al. (2017). Preparation and evaluation of self-microemulsions for improved bioavailability of ginsenoside-Rh1 and Rh2. *Drug Deliv Transl Res* 7:731–7.
- Yang L, Xin J, Zhang Z, et al. (2016). TPGS-modified liposomes for the delivery of ginsenoside compound K against non-small cell lung cancer: formulation design and its evaluation in vitro and in vivo. *J Pharm Pharmacol* 68:1109–18.
- Yang L, Zhang Z, Hou J, et al. (2017). Targeted delivery of ginsenoside compound K using TPGS/PEG-PCL mixed micelles for effective treatment of lung cancer. *IJN* 12:7653–67.
- Yang Z, Zhao T, Liu H, et al. (2016). Ginsenoside Rh2 inhibits hepatocellular carcinoma through  $\beta$ -catenin and autophagy. *Sci Rep* 6:19383
- Zare-Zardini H, Taheri-Kafrani A, Amiri A, Bordbar AK. (2018). New generation of drug delivery systems based on ginsenoside Rh2-, lysine- and arginine-treated highly porous graphene for improving anticancer activity. *Sci Rep* 8:586.
- Zhang X, Tang W, Yang Z, et al. (2014). PEGylated poly(amine-co-ester) micelles as biodegradable non-viral gene vectors with enhanced stability, reduced toxicity and higher in vivo transfection efficacy. *J Mater Chem B* 2:4034–44.
- Zhuang J, Yin J, Xu C, et al. (2018). 20(S)-ginsenoside Rh2 induce the apoptosis and autophagy in U937 and K562 cells. *Nutrients* 10:328.